NISTIR 6310

Modeling of Bare and Aspirated Thermocouples in Compartment Fires

Linda G. Blevins and William M. Pitts

Building and Fire Research Laboratory
Gaithersburg, Maryland 20899

United States Department of Commerce
Technology Administration
National Institute of Standards and Technology

NISTIR 6310

Modeling of Bare and Aspirated Thermocouples in Compartment Fires

Linda G. Blevins and William M. Pitts

April, 1999
Building and Fire Research Laboratory
National Institute of Standards and Technology
Gaithersburg, MD 20899

U.S. Department of Commerce
William M. Daley, *Secretary*
Technology Administration
Gary Bachula, *Acting Under Secretary for Technology*
National Institute of Standards and Technology
Raymond G. Kammer, *Director*

ABSTRACT

As part of an effort to characterize the uncertainties associated with temperature measurements in fire environments, models of bare bead, single-shielded aspirated, and double-shielded aspirated thermocouples were developed and used to study the effects of varying the gas and average effective surroundings temperatures on the thermocouple error of each configuration. The models indicate that thermocouples respond differently to changes in effective surroundings temperature in a hot upper layer than in a relatively cooler lower layer of a room fire. In an upper layer, for a given gas temperature, the thermocouple error is relatively insensitive to surroundings temperature. In a lower layer, errors which increase rapidly with surroundings temperature are possible. The most extreme errors occur in a lower layer when the gas temperature is low and the surroundings temperature is high. Aspirated thermocouples reduce the errors in both the upper and lower layers of a room fire, but do not eliminate them entirely. The present study is intended to provide fire researchers with a methodology for developing working models of thermocouples which are tailored to their own configurations.

NOTATION

A_j, A_k	Surface area of arbitrary surface j or k (m^2)
A_b	Surface area of thermocouple bead (m^2)
A_c	Annular flow area of double-shielded probe (m^2)
A_i	Surface area of the innermost shield for double-shielded probe (m^2)
A_o	Surface area of outermost shield for single- and double-shielded probes (m^2)
$C_{i\to o}$	Geometric constant defined for double-shielded model
D_{char}	Characteristic length used for defining Nusselt number (m)
D_b	Thermocouple bead diameter (m)
D_h	Hydraulic diameter of annular region of double-shielded probe (m)
D_i	Innermost shield diameter for double-shielded probe (m)
D_o	Outermost shield diameter for single- and double-shielded probes (m)
F_{jk}	Radiation configuration factor between surfaces j and k
h_{bU}	Convective heat transfer coefficient between external gas flow and bare thermocouple bead ($W/m^2 \cdot K$)
h_{bu}	Convective heat transfer coefficient between aspirating gas flow and thermocouple bead for single- and double-shielded probes ($W/m^2 \cdot K$)
h_{iu}	Convective heat transfer coefficient between aspirating gas flow and innermost shield for double-shielded probe ($W/m^2 \cdot K$)
h_{iw}	Convective heat transfer coefficient between annular aspirating gas flow and innermost shield for double-shielded probe ($W/m^2 \cdot K$)
h_{jv}	Convective heat transfer coefficient between gas with velocity v and arbitrary surface j ($W/m^2 \cdot K$)
h_{ou}	Convective heat transfer coefficient between aspirating gas flow and shield for single-shielded probe ($W/m^2 \cdot K$)
h_{oU}	Convective heat transfer coefficient between external gas flow and outermost shield for single- and double-shielded probes ($W/m^2 \cdot K$)
h_{ow}	Convective heat transfer coefficient between annular aspirating gas flow and outermost shield for double-shielded probe ($W/m^2 \cdot K$)
k_g	Gas thermal conductivity ($W/m \cdot K$)
L	Distance from probe inlet to thermocouple bead for single- and double-shielded probes (m)
Nu_{jv}	Nusselt number for gas with velocity v and arbitrary surface j

P_w	Wetted perimeter of annulus for double shielded probe (m)
$q_{\text{rad}\,j\to k}$	Rate of radiative heat transfer from surface j to surface k (W)
$q_{\text{conv}\,j,\,v}$	Rate of convective heat transfer from a gas with velocity v to surface j (W)
T_b	Thermocouple bead temperature (°C or K)
T_g	Gas temperature (°C or K)
T_i	Innermost shield temperature for double-shielded probe (°C or K)
T_j, T_k	Temperature of arbitrary surface j or k (°C or K)
T_o	Outermost shield temperature for single- and double-shielded probes (°C or K)
T_∞	Average effective surroundings temperature (°C or K)
u	Aspiration velocity across thermocouple bead for single and double-shielded probes (m/s)
U	External fire-induced flow velocity (m/s)
w	Aspiration velocity in the annulus for double-shielded probe (m/s)
ΔT	Thermocouple error (°C or K)
ε_b	Thermocouple bead emissivity
ε_o	Outermost shield emissivity for single- and double-shielded probes
ε_i	Innermost shield emissivity for double-shielded probe
ε_j, ε_k	Emissivity of arbitrary surface j or k
σ	Stefan-Boltzmann constant (5.67×10^{-8} W/m^2·K^4)

1 INTRODUCTION

Measuring gas temperature in and around fires is important for verifying and validating computer models and for gaining an empirical understanding of complex fire behavior. The most common way to measure temperature during fire testing is to use bare thermocouples. However, the temperature indicated by a bare thermocouple near an enclosure fire differs from the true gas temperature because the bead exchanges radiation with the room walls, the hot flame gases and soot, and the ambient environment through doors and windows. Radiation corrections are difficult to perform during fire testing for several reasons. First, selecting an effective surroundings temperature is arduous because of the temporally and spatially varying environment. In addition, the local convection velocity and gas composition vary and are not usually known. The emissivity of the thermocouple bead varies with temperature and with exposure to fire environments; soot can accumulate, changing the bead diameter and its thermophysical properties. Finally, convective heat transfer correlations are based on experiments and have high uncertainties [1]. Because of these difficulties, fire researchers often perform experiments without considering radiation losses or gains on thermocouples. Unfortunately, this procedure can yield ambiguous gas temperature readings [2,3]. NIST is presently working to characterize experimentally these ambiguities [4]. The present paper describes idealized heat transfer modeling of thermocouples in fire environments performed in support of the NIST effort.

One way to reduce the effect of external radiative exchange on a thermocouple measurement is to use an aspirated thermocouple, which consists of a thermocouple enclosed in one or more cylindrical radiation shields. The gas to be measured is pulled axially through the shield(s) using a pump or other aspiration device. The shield(s) reduce the radiative exchange between the thermocouple and its surroundings, while the rapid flow increases the convective exchange between the gas and the thermocouple. The result is that the temperature indicated by an aspirated thermocouple is closer to the true gas temperature than that indicated by a bare thermocouple of similar bead size.

While using an aspirated thermocouple favorably reduces the influence of radiation on the measurement, temporal and spatial resolution are sacrificed. In addition, aspirated thermocouples are cumbersome. For example, during a recent NIST study, a large ice bath, two dry carbon dioxide traps, and two glass wool filters were necessary in each aspirated thermocouple sampling line to protect the vacuum pump and rotameter from water damage and soot clogging [4]. This is especially constraining when many thermocouples are used simultaneously, which is generally desirable for fire studies. Because aspirated thermocouples involve tradeoffs in resolution and ease of use, the individual researcher must decide if the improvements offered by their use justify the extra effort to use them.

The goal of the present research was to use idealized modeling to elucidate the ways that bare and aspirated thermocouples respond to the thermal environments present in fires. The behaviors of thermocouples exposed to conditions characteristic of upper and lower layers of a room fire were predicted. The modeling was performed to help researchers (1) make informed thermocouple choices when planning experiments, and (2) understand the uncertainties in thermocouple measurements while and after they are made.

Several papers have been published on the design and use of aspirated thermocouples, also known as "suction pyrometers," in furnaces, gas turbines, and other combustion environments [5-22]. These works generally emphasize applications where (1) the temperature of the surrounding walls is lower than the temperature of the gas, and (2) the gas and surroundings temperature do not differ appreciably (but are large enough to warrant concern). In a room fire, which often consists of a relatively cool lower gas layer and a generally hot upper gas layer, these two conditions are not always satisfied. Hence, examination of aspirated thermocouples in *fire* environments is warranted. To the authors' knowledge, Newman and Croce published the only study focusing on the design of aspirated thermocouples for fire research [23]. They developed a prototype aspirated thermocouple which featured a 1.8-mm-diameter thermocouple bead enclosed in a 6.4-mm-diameter steel shield. Newman and Croce tested their instrument by increasing the flow through the probe until the measured temperature approached a value which seemed independent of aspiration velocity. Based on this technique, they concluded that an aspiration velocity of about 7 m/s was adequate to obtain a temperature "which should correspond to the true gas temperature [23]." The American Society for Testing and Materials (ASTM), in the *Standard Guide for Room Fire Experiments*, similarly recommends that the aspiration velocity be maintained near 5 m/s, stating that this is "sufficiently high to allow accurate temperature measurement based on thermocouple voltage alone, even within flame zones [24]." Luo, in a recent paper addressing radiation effects on thermocouples in fires, stated that the use of an aspirated thermocouple with a 2-m/s aspiration velocity "gives the true gas temperature [3]." In contrast, previously published studies of aspirated thermocouples recommend aspiration velocities between 100 m/s and 300 m/s [5]. This contradiction in recommended aspiration velocity is addressed during the present work.

Heat transfer models for bare-bead, single-shielded aspirated, and double-shielded aspirated thermocouples are described in this paper. Modeling results are used to (1) demonstrate that thermocouples behave differently in the upper and lower layers of a room fire, (2) establish the potential for aspirated thermocouples to reduce errors in room fire temperature measurements, and (3) illustrate that the ASTM-recommended 5-m/s aspiration velocity is not always fast enough to obtain accurate measurements around fires.

2 MODEL DEVELOPMENT

The bare-bead, single-shielded aspirated, and double-shielded aspirated thermocouple models were developed using steady-state, combined-mode heat transfer analysis with graybody-enclosure radiative exchange [25]. Important model development details are summarized here. Full derivations of the equations are given elsewhere [4]. The graybody enclosure analysis involves assuming that all surfaces are isothermal and opaque, and that they possess absorptivities and emissivities which are independent of wavelength and temperature. It also involves assuming that all emitted, reflected, and incident radiation has the same intensity in all directions. Arguments for the appropriateness of the graybody enclosure analysis are available [26].

For the purpose of capturing the basic physics of a thermocouple responding to its environment, it is assumed that heat is added to or removed from the surroundings in an unspecified amount which allows them to remain at a constant effective temperature, T_∞. The surroundings

temperature T_∞ represents the effective radiation temperature of the potentially multi-temperature surrounding environment. It does not represent the temperature of any single object in a room; rather, it can be thought of as the temperature of an imaginary enclosure which would exchange radiation with the thermocouple at a rate equivalent to the net radiative exchange rate experienced by the thermocouple in its multi-object environment.

All gases are assumed to be isothermal for the present analysis. Neglecting temperature gradients in gases and on surfaces should not affect the general behavioral trends presented in this paper; including them would immensely complicate the formulation. The thermophysical properties of the gases are assumed to be those of air, calculated using polynomial curve fits of tabulated values [27]. This is reasonable since air (composed mostly of nitrogen) is a constituent of most fire gases. Consistent with previous experimental findings [28], a fire-induced gas flow, with a velocity of U, is assumed to exist in the vicinity of the thermocouple. Gases are assumed to be radiatively non-participating, which is valid for small optical depths. For large optical depths, hot gas and/or soot may partially or fully attenuate radiative exchange between a thermocouple and its surroundings; hence, if a thermocouple is immersed in an optically thick region of a fire, the present models do not apply [4]. For the aspirated thermocouple models, radiative exchange between the thermocouple bead and its local surroundings through its shield opening is neglected. This assumption is valid *only* if the shield opening faces a region with a temperature similar to the shield temperature. In reality, radiative exchange through the opening during a fire can alter the effectiveness of an aspirated thermocouple [4]. While the magnitude of the predicted errors will be affected by this type of exchange, the behavioral trends predicted here should not.

All radiation interchange is modeled as two-body exchange (i.e., each surface 'sees' only one other surface). Hence, the radiative heat transfer between surfaces j and k is written as [27]

$$q_{\text{rad } j\to k} = \frac{\left(\sigma T_j^{\,4} - \sigma T_k^{\,4}\right)}{\dfrac{1-\varepsilon_j}{\varepsilon_j A_j} + \dfrac{1}{F_{jk} A_j} + \dfrac{1-\varepsilon_k}{\varepsilon_k A_k}}, \tag{1}$$

where F_{jk} is the fraction of radiant energy leaving surface j which strikes surface k. This equation is valid if surface j is completely enclosed in surface k. If surface j is convex (F_{jk}=1) and has much smaller area than surface k (A_j/A_k<<1), then Eq. (1) reduces to

$$q_{\text{rad } j\to k} = \varepsilon_j A_j \left(\sigma T_j^{\,4} - \sigma T_k^{\,4}\right). \tag{2}$$

If surface j is convex and has an area which is comparable to the area of surface k, then Eq. (1) reduces to

$$q_{\text{rad } j\to k} = \frac{A_j\left(\sigma T_j^{\,4} - \sigma T_k^{\,4}\right)}{\dfrac{1}{\varepsilon_j} + \dfrac{1-\varepsilon_k}{\varepsilon_k}\left(\dfrac{A_j}{A_k}\right)}. \tag{3}$$

All convective heat transfer is modeled using Newton's law of cooling, which for convection from a gas with a velocity v to a surface j is written as [27]

$$q_{\text{conv } j,v} = h_{jv} A_j \left(T_g - T_j\right). \tag{4}$$

The convective heat transfer coefficients are calculated using correlations developed for the Nusselt number, defined for surface j and gas velocity v as [27]

$$Nu_{jv} = \frac{h_{jv} D_{\text{char}}}{k_g}. \tag{5}$$

The characteristic length, D_{char}, is defined based on the geometry of interest. The conductivity, k_g, is evaluated either at T_g or at the average of the gas and solid temperatures, depending on the convention defined when the correlation of interest was developed [1,27].

The governing equations were kept in dimensional form for the present study. While nondimensionalization minimizes the number of parameters to be varied when analyzing a problem, it proves to be difficult when equations have both fourth-order and first-order terms, and when heat transfer correlations depend on local conditions in a complex way. Keeping the model equations in dimensional form allows the present study to be focused on regions of room fires (upper and lower layers) which are physically identifiable using reasonable values of the gas and surroundings temperatures.

The thermocouple error, ΔT, used to evaluate a particular thermocouple's effectiveness, is defined as the absolute value of the difference between the thermocouple bead temperature and the true gas temperature,

$$\Delta T = \left|T_b - T_g\right|. \tag{6}$$

It is important to note that the absolute magnitudes of the thermocouple errors reported in this paper are strong functions of the particular modeling parameters selected. Hence the reader should focus on the *trends* described rather than on the absolute errors. These trends provide useful general information about the behavior of thermocouples in fire environments, and they provide insight into performance differences between bare bead, single-shielded aspirated, and double-shielded aspirated configurations in upper and lower layers of room fires.

Probe and bead sizes were selected to closely match those used in recent NIST experiments [4]. The baseline parameters were aspiration velocity $u = 5$ m/s (recommended by ASTM [24]), emissivities $\varepsilon_b = \varepsilon_O = \varepsilon_i = 0.8$ (typical values for dull, oxidized metal [27]), fire-induced flow

velocity $U = 0.5$ m/s (typically 0-2 m/s in enclosure fires [28]), and bead diameter $D_b = 1.5$ mm (three times wire diameter [29,30]). A thermocouple wire diameter of 0.5 mm was used for rigidity in the aspirated probes [4]. The same wire diameter (and resulting large 1.5-mm bead) was used for the bare-bead calculations presented here for direct comparison with aspirated-thermocouple results.

This paper presents two parametric studies. First, solutions for thermocouples exposed to various combinations of T_g and T_∞ are given. Second, solutions for a single-shielded aspirated thermocouple operating with various aspiration velocities are presented. Detailed results of a full parametric study are described elsewhere [4].

It should be noted that the modeling presented here does not include transient effects. This is limiting because the temperature indicated by a thermocouple is a complex function of its temporal response behavior, the rate of change of both T_g and T_∞, and the time constants of radiative and convective heat transfer. However, the present steady-state modeling can be used to understand the driving forces behind this transient behavior, and may be used as a building block for future transient characterization efforts.

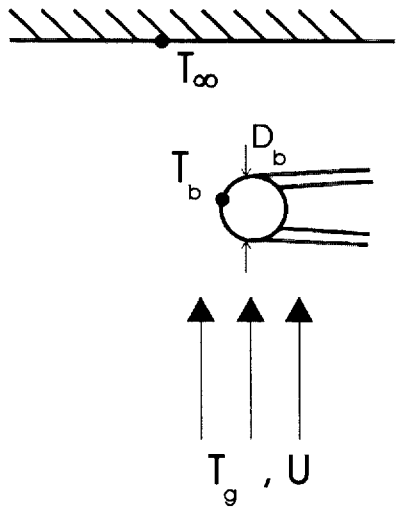

Fig. 1 Schematic of bare thermocouple bead.

2.1 Bare-Bead Model Equations

A schematic (not to scale) of the bare-bead thermocouple is shown in Fig. 1. Heat is transferred to or from the bead via convection and radiation. Radiative exchange between the bead and surroundings can be modeled by Eq. (2). The energy balance on the bead then yields

$$h_{bU}\left(T_g - T_b\right) = \varepsilon_b \sigma \left(T_b^4 - T_\infty^4\right), \tag{7}$$

or

$$T_b^4\left[\varepsilon_b \sigma\right] + T_b\left[h_{bU}\right] - \left[\varepsilon_b \sigma T_\infty^4 + h_{bU} T_g\right] = 0. \tag{8}$$

The convective heat transfer coefficient between the external gas flow and the thermocouple bead, h_{bU}, is estimated using Whitaker's correlation for external flow over a sphere [1]. Calculated Nusselt numbers based on D_b and U are accurate to within ±25% (no coverage factor provided) [1]. For a given gas temperature and surroundings temperature, Eq. (8) is solved for the thermocouple temperature, T_b, using a first order Newton's method.

2.2 Single-Shield Model Equations

A schematic (not to scale) of the single-shielded aspirated thermocouple is shown in Fig. 2. Convection to the thermocouple bead takes place on its outside surface, while convection to the shield takes place on both its inside and outside surfaces. Radiative exchange between the thermocouple bead and the inner surface of the shield, and between the outer surface of the shield and the surroundings, are modeled using Eq. (2). The energy balances on the bead and shield, respectively, become

$$h_{bu}\left(T_g - T_b\right) = \varepsilon_b \sigma\left(T_b^4 - T_o^4\right), \tag{9}$$

and

$$h_{ou}\left(T_g - T_o\right) + h_{oU}\left(T_g - T_o\right) = -\varepsilon_b \sigma\left(\frac{A_b}{A_o}\right)\left(T_b^4 - T_o^4\right) + \varepsilon_o \sigma\left(T_o^4 - T_\infty^4\right). \tag{10}$$

These may be simplified and written in final form as

$$T_b^4\left[\varepsilon_b \sigma\right] + T_b\left[h_{bu}\right] - \left[\varepsilon_b \sigma T_o^4 + h_{bu} T_g\right] = 0, \tag{11}$$

and

$$T_o^4\left[\varepsilon_o \sigma\right] + T_o\left[h_{ou} + h_{oU}\right] - \left[\varepsilon_o \sigma T_\infty^4 + \left(h_{ou} + h_{oU}\right) T_g\right] = 0. \tag{12}$$

The convective heat transfer coefficient between the aspirating gas flow and the thermocouple bead, h_{bu}, is estimated using a correlation for a sphere of diameter D_b with a crossflow velocity equal to the aspiration velocity u, yielding a Nusselt number accurate within ±25% (no coverage factor provided) [1]. The convective heat transfer coefficient between the aspirating gas and the shield, h_{ou}, is computed using a correlation for either developing laminar or fully turbulent flow, with Nusselt numbers based on D_o and u. For developing laminar flow, the Seider-Tate correlation for combined entry lengths is used [27]. This correlation is valid for cylinders with uniform wall temperature, yielding Nusselt numbers which are accurate to within ±25% (no coverage factor provided) [27]. For turbulent flow, h_{ou} is computed using the correlation developed by Petukhov, Kirillov, and Popov, and modified by Gnielinski [27], with the friction factor defined for smooth tubes. Nusselt numbers calculated using this equation are accurate to within ±10% (no coverage factor provided) [27]. When varying the aspirating velocity from 0 m/s upward, the correlation for developing flow is applied until the aspiration velocity is reached for which the predicted thermocouple temperature equals that obtained using the turbulent flow correlation. For velocities larger than this, the turbulent flow correlation is used to compute the heat transfer

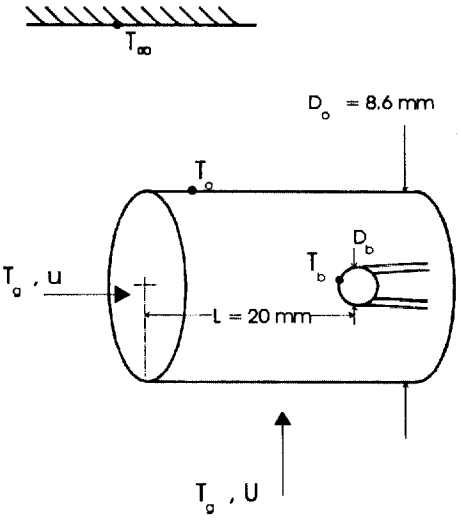

Fig. 2 Schematic of single-shielded aspirated thermocouple.

coefficient. The convective heat transfer coefficient between the external gas stream and the shield, h_{oU}, is estimated using the Churchill and Bernstein correlation for a cylinder in crossflow, yielding Nusselt numbers based on D_o and U accurate to within ±25% (no coverage factor provided) [27].

For a given T_g and T_∞, Eq. (12) is solved for T_o using a first order Newton's method. Using this result, Eq. (11) is subsequently solved for T_b in similar fashion. When there is no aspiration, the bead and shield equilibrate at a common temperature.

2.3 Double-Shield Model Equations

A schematic (not to scale) of the double-shielded aspirated thermocouple is shown in Fig. 3. The double-shielded probe is identical to the single-shielded probe with an inner shield added. Radiative exchange between the thermocouple bead and the inner surface of the inner shield, and between the outer surface of the outer shield and the surroundings, are modeled using Eq. (2). Because the area of the inner shield is *not* significantly smaller than the area of the outer shield, the rate of radiative exchange between the outer surface of the inner shield and the inner surface of the outer shield is described by Eq. (3). If the constant $C_{i\to o}$ is defined such that

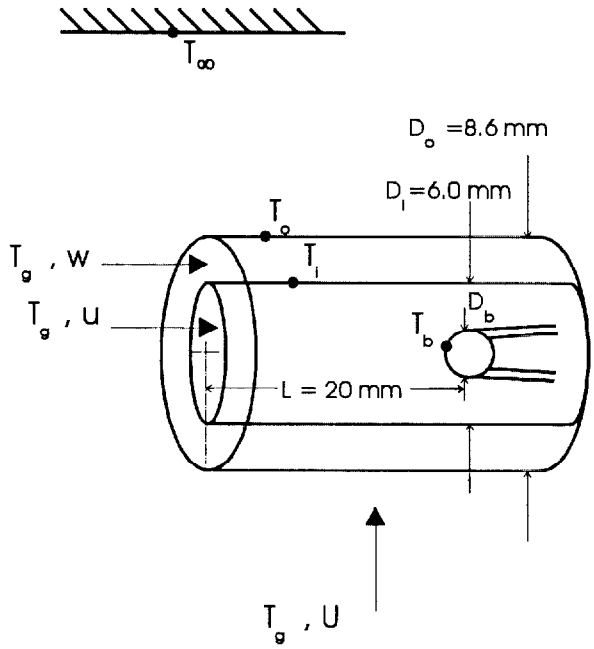

Fig. 3 Schematic of double-shielded aspirated thermocouple.

$$C_{i\to o} = \frac{1}{\frac{1}{\varepsilon_i} + \frac{1-\varepsilon_o}{\varepsilon_o}\left(\frac{A_i}{A_o}\right)}, \tag{13}$$

then the energy balances for the bead, inner shield, and outer shield, respectively, become

$$h_{bu}\left(T_g - T_b\right) = \varepsilon_b \sigma\left(T_b^4 - T_i^4\right), \tag{14}$$

$$h_{iu}\left(T_g - T_i\right) + h_{iw}\left(T_g - T_i\right) = -\varepsilon_i \sigma\left(\frac{A_b}{A_i}\right)\left(T_b^4 - T_i^4\right) + C_{i\to o}\sigma\left(T_i^4 - T_o^4\right), \tag{15}$$

and

$$h_{ow}\left(T_g - T_o\right) + h_{oU}\left(T_g - T_o\right) = -C_{i\to o}\sigma\left(\frac{A_i}{A_o}\right)\left(T_i^4 - T_o^4\right) + \varepsilon_o \sigma\left(T_o^4 - T_\infty^4\right). \tag{16}$$

In final form, these equations are written as

$$T_b^4\left[\varepsilon_b\sigma\right]+T_b\left[h_{bu}\right]-\left[\varepsilon_b\sigma T_i^4+h_{bu}T_g\right]=0, \tag{17}$$

$$T_i^4\left[C_{i\to o}\sigma\right]+T_i\left[\left(h_{iu}+h_{iw}\right)\right]-\left[C_{i\to o}\sigma T_o^4+\left(h_{iu}+h_{iw}\right)T_g\right]=0, \tag{18}$$

$$T_o^4\left[C_{i\to o}\sigma\left(A_i/A_o\right)+\varepsilon_o\sigma\right]+T_o\left[\left(h_{ow}+h_{oU}\right)\right]- \tag{19}$$

and

$$\left[C_{i\to o}\sigma\left(A_i/A_o\right)T_i^4+\varepsilon_o\sigma T_\infty^4+\left(h_{ow}+h_{oU}\right)T_g\right]=0.$$

The convective heat transfer coefficient between the aspirating gas flow and the thermocouple bead, h_{bu}, and that between the external gas stream and the outer shield, h_{oU}, are calculated as for the single-shielded probe. The heat transfer coefficient between the internal gas flow and the inner shield, h_{iu}, is estimated using the developing and turbulent pipe flow correlations (described previously) based on D_i and u. In the annulus, h_{iw} and h_{ow} are considered equal, and are calculated using the developing and turbulent pipe flow correlations based on the hydraulic diameter, D_h [27]. It is customary to define the hydraulic diameter as four times the ratio of the flow area (A_c) to the wetted perimeter (P_w) [27],

$$D_h=\frac{4A_c}{P_w}=\frac{4(\pi/4)\left(D_o^2-D_i^2\right)}{\pi D_o+\pi D_i}=D_o-D_i. \tag{20}$$

The gas velocity in the annulus (w) is assumed to be equal to that through the innermost shield (u) for all results reported here.

For a given T_g and T_∞, Eqs. (17), (18), and (19) are solved simultaneously for T_b, T_i, and T_o using nested Newton's methods. When there is no aspiration, the bead and both shields equilibrate at a common temperature.

3 RESULTS AND DISCUSSION

3.1 Effect of Gas and Surroundings Temperatures

Figure 4 depicts the temperature error, ΔT, predicted for a 1.5-mm bare-bead thermocouple, as a function of T_∞, for gas temperatures of 27 °C (300 K), 127 °C (400 K), 377 °C (650 K), 627 °C (900 K), and 877 °C (1150 K), and 1127 °C (1400 K). For these calculations, $\varepsilon_b = 0.8$ and $U = 0.5$ m/s. The region where T_g is higher than T_∞ is termed the "upper layer," recognizing that the region includes but is not limited to the conditions generally found in the upper layer of a room fire. Similarly, the region where T_g is lower than T_∞ is termed the "lower layer." The ovals are printed on the figure to indicate that upper layer ($T_g > T_\infty$) conditions generally occur on the left side of the graph and lower layer ($T_g < T_\infty$) conditions occur on the right side. Figure 4 shows that a bare bead thermocouple behaves differently in the upper and lower layers of a room fire. In

the upper layer, the thermocouple indicates a temperature which is lower than T_g. The upper layer thermocouple error for a given T_g is relatively insensitive to T_∞, decreasing gradually to zero as T_∞ approaches T_g. In this region, the thermocouple error increases with increasing T_g. In contrast, in the lower layer, the thermocouple indicates a temperature which is higher than T_g. The lower layer thermocouple error is a strong function of both T_g and T_∞, increasing more and more rapidly with increasing T_∞ when the latter value is relatively high. In this region, the thermocouple error decreases with increasing T_g. The behavior in both regions is controlled by the fourth order dependence of the radiative heat transfer rate on T_∞. The most extreme errors (hundreds of degrees) occur in the lower layer when T_g is at its lowest assumed value (27 °C) and T_∞ is at its highest (1127 °C), which would most likely be encountered only during a fully-involved room fire. These modeling results are consistent with experimental findings that errors of greater than 100 °C are possible when bare thermocouples are used in fire environments, and that lower-layer errors are more extreme than upper-layer errors [3].

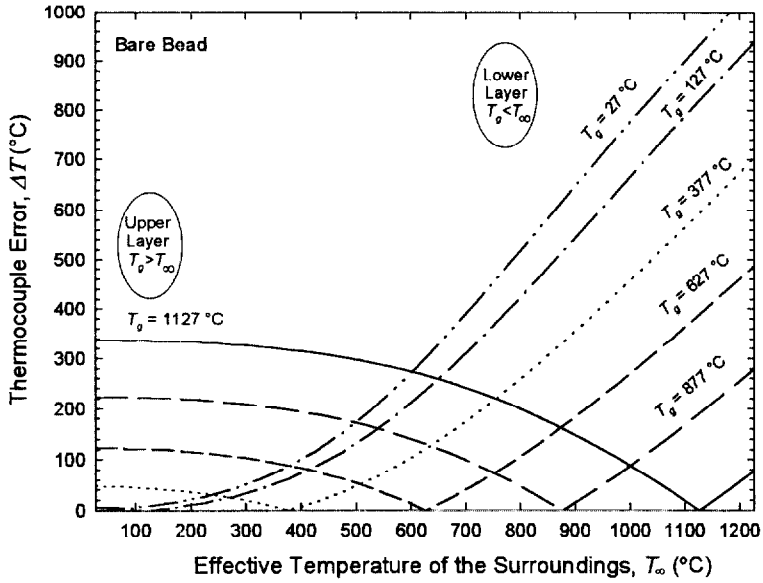

Fig. 4 Effect of surroundings temperature on error in measured temperature for a bare bead thermocouple with diameter D_b = 1.5 mm, emissivity ε_b = 0.8, and external flow velocity U = 0.5 m/s, and gas temperatures of 27 °C, 127 °C, 377 °C, 627 °C, 877 °C, and 1127 °C. The surroundings temperature is that of an imaginary, isothermal enclosure which would exchange radiation with the thermocouple at a rate equivalent to the actual rate it experiences.

Figure 5 depicts the predicted temperature error for the single-shielded thermocouple. For these calculations, u = 5 m/s, $\varepsilon_b = \varepsilon_o$ = 0.8, D_b = 1.5 mm, and U = 0.5 m/s. Figure 5 demonstrates that the single-shielded probe behaves similarly to the 1.5 mm bare-bead thermocouple, except the errors in the upper and lower layers are reduced for a given T_g and T_∞, and the region of rapidly

increasing error in the lower layer is shifted to higher T_∞. This shift is expected to decrease the likelihood that the region of high error will be encountered in an actual room fire test. This conjecture is based on the assumption that the amount of time for which a thermocouple placed in the lower layer will experience a given T_∞ decreases as T_∞ increases to 1100 °C and above. The figure shows that the temperature error of the single-shielded thermocouple has an upper bound at about 190 °C for T_g = 1127 °C in the upper layer, which is about half of the 340 °C upper bound error for the bare bead thermocouple for the same T_g. Similar trends occur for the other conditions considered in the figure. Thus, the single shield reduces the bare-bead thermocouple error to about half of its value in the upper layer, and decreases the likelihood that large errors will occur in the lower layer.

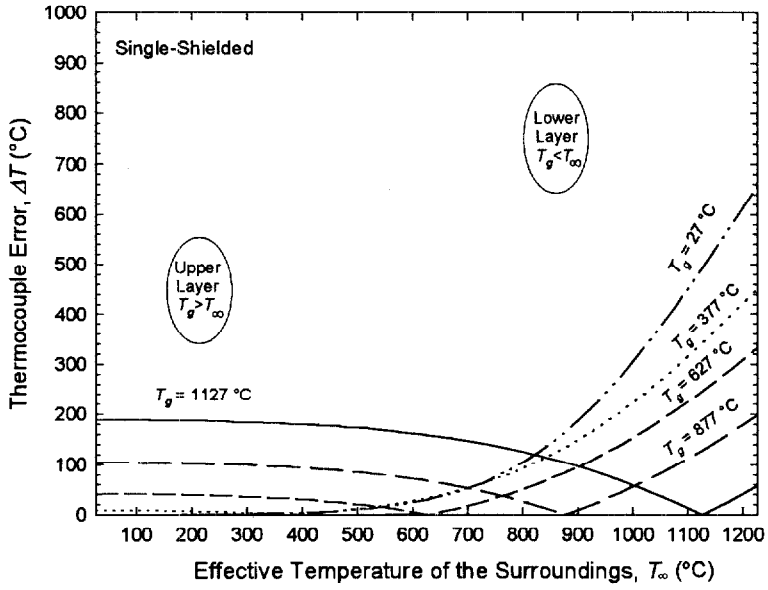

Fig. 5 Effect of surroundings temperature on error in measured temperature for a single-shielded aspirated thermocouple, with bead diameter D_b = 1.5 mm, shield diameter D_o = 8.6 mm, emissivities $\varepsilon_b = \varepsilon_o$ = 0.8, external velocity U = 0.5 m/s, aspiration velocity u = 5 m/s, and gas temperatures of 27 °C, 377 °C, 627 °C, 877 °C, and 1127 °C.

Figure 6 depicts the temperature error for the double-shielded thermocouple. The range of the ordinate axis is half that of the ordinate axes in Figs. 4 and 5. For these calculations, u = 5 m/s, w = 5 m/s, $\varepsilon_b = \varepsilon_o = \varepsilon_i$ = 0.8, D_b = 1.5 mm, and U = 0.5 m/s. The figure shows that the double-shielded thermocouple behaves similarly to the single-shielded thermocouple, except that errors in the upper and lower layers are reduced further, and the region of rapidly increasing error in the lower layer is shifted to even higher T_∞. This shift dramatically decreases the likelihood that extreme errors will occur in the lower layer, since the shift is toward unrealistically high values of T_∞ for typical room fires. Subject to the present modeling assumptions, the upper layer error for the double-shielded probe has an upper bound at 100 °C for T_g = 1127 °C, which is about half of the 190 °C bound of the single-shielded thermocouple exposed to the same conditions. Similar

trends occur for the other conditions considered in the figure. Thus, the double-shielded probe represents a significant improvement over the single-shielded probe, both in the upper layer where the errors are decreased to about half of their single-shield values, and in the lower layer where errors are reduced and the likelihood of occurrence of large errors is lessened. The improved performance of the double-shielded probe results from better radiation shielding and from higher convective heat transfer rates effected by the rapid flow through the annulus.

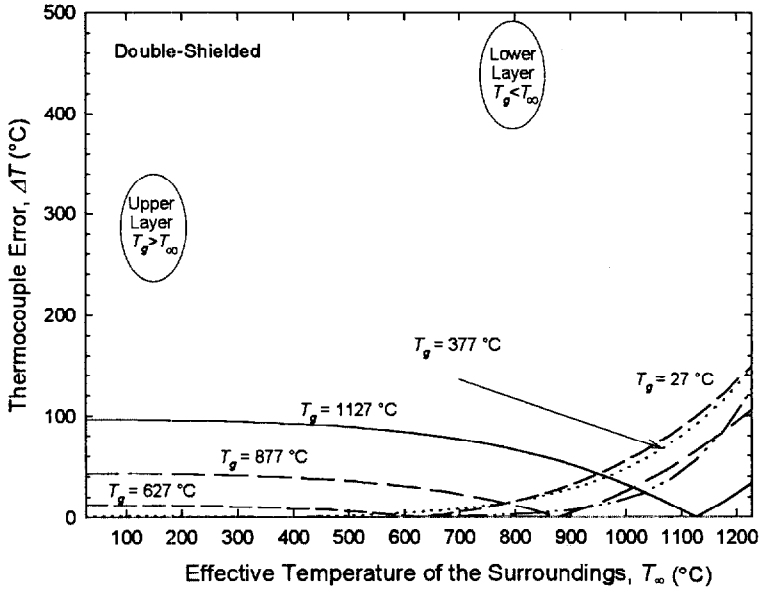

Fig. 6 Effect of surroundings temperature on error in measured temperature for a double-shielded aspirated thermocouple, with bead diameter D_b = 1.5 mm, inner shield diameter D_i = 6.0 mm, outer shield diameter D_o = 8.6 mm, emissivities $\varepsilon_b = \varepsilon_i = \varepsilon_o$ = 0.8, external velocity U = 0.5 m/s, and aspiration velocities u = 5 m/s and w = 5 m/s, and gas temperatures of 27 °C, 377 °C, 627 °C, 877 °C, and 1127 °C.

The results presented in this section reveal that lower layer thermocouple errors are generally very sensitive to T_∞ for a given T_g. A small change in a fire can hence cause a very large change in the temperature indicated by a lower layer thermocouple. Even aspirated thermocouples are susceptible to this radiation effect. It is worth mentioning that the T_∞ experienced by a thermocouple in any region of an enclosure fire generally increases as the fire grows. Hence, lower-layer thermocouple errors are likely to be low initially but increase in magnitude as time (and fire growth) progresses. Near flashover, room fire conditions change so rapidly that application of the present (or any other) model becomes extremely difficult.

One benefit of solving the types of equations developed here is that unusual data trends can be explained. For example, thermocouples used at floor level in the doorway of an enclosure should indicate ambient temperature since there is no preheat mechanism for the incoming air [28]. However, bare thermocouples used in these locations often indicate temperatures higher than

room temperature [3,28]. Considering that lower layer thermocouples are very susceptible to radiation errors of the type depicted on the right side of Fig. 4, this experimental result is not surprising.

3.2 Effect of Aspiration Velocity

To demonstrate the role of aspiration velocity on the effectiveness of a single-shielded aspirated thermocouple, Figs. 7, 8, and 9 depict its predicted response to changes in this velocity for selected upper and lower layer cases. A vertical line on each figure marks the 5-m/s aspiration velocity recommended for use with single-shielded thermocouples by ASTM. Horizontal lines on each figure mark the values of the gas and surroundings temperatures.

Figure 7 shows predictions for selected upper and lower layer cases when the difference between T_g and T_∞ is 900 °C. Results for an upper layer case with $T_g = 927$ °C and $T_\infty = 27$ °C are shown along with predictions for a lower layer case with these values transposed ($T_g = 27$ °C and $T_\infty = 927$ °C). These cases represent *extreme* but perhaps not impossible gas and surroundings temperature differences for a fire. As aspiration velocity is increased, the upper layer thermocouple temperature increases suddenly from its no-aspiration value of 450 °C to 730 °C, and then rises gradually toward T_g (927 °C). The lower-layer thermocouple temperature drops from its no-aspiration value of 860 °C to 690 °C and then gradually approaches T_g (27 °C) as aspiration velocity is increased. Hence, T_b approaches T_g asymptotically as u is increased.

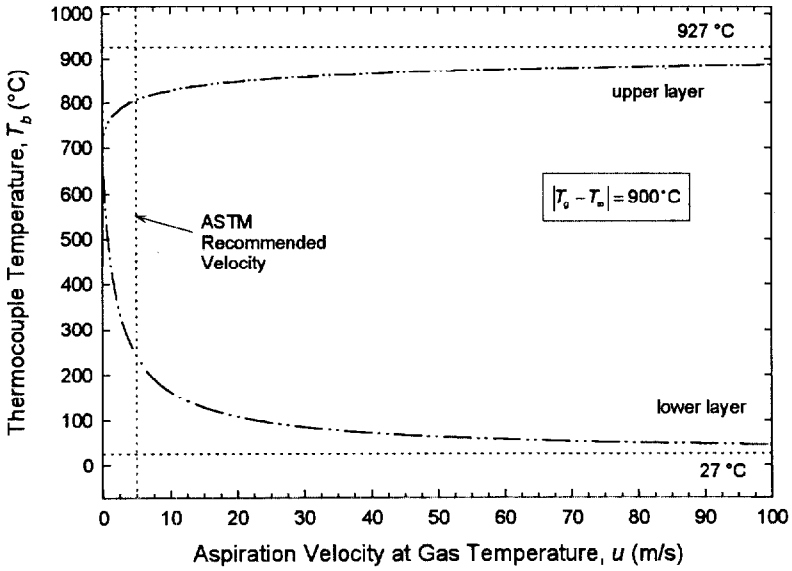

Fig. 7 Predicted single-shielded thermocouple response to variation in aspiration velocity for conditions with differences between T_g and T_∞ of 900 °C. The upper layer case corresponds to $T_g = 927$ °C and $T_\infty = 27$ °C, and the lower layer case corresponds to $T_g = 27$ °C and $T_\infty = 927$ °C. The vertical line denotes the ASTM-recommended 5-m/s aspiration velocity, and horizontal lines mark the important temperatures of 27 °C and 927 °C.

Figure 8 shows predictions for selected upper and lower layer cases when the difference between T_g and T_∞ is 600 °C. Results for an upper layer case with $T_g = 627$ °C and $T_\infty = 27$ °C are shown along with predictions for a lower layer case with $T_g = 27$ °C and $T_\infty = 627$ °C. These scenarios represent *moderate* gas and surroundings temperature differences which might occur during fire growth. As aspiration velocity is increased, the upper layer thermocouple temperature increases suddenly from its no-aspiration value of 360 °C to 530 °C, and then rises gradually toward T_g (627 °C). The lower layer thermocouple temperature drops from its no-aspiration value of 520 °C to 270 °C, and subsequently approaches T_g (27 °C). For the $|T_g - T_\infty| = 600°C$ curves shown in the figure, T_b approaches T_g more rapidly than for the $|T_g - T_\infty| = 900°C$ curves shown in Fig. 7.

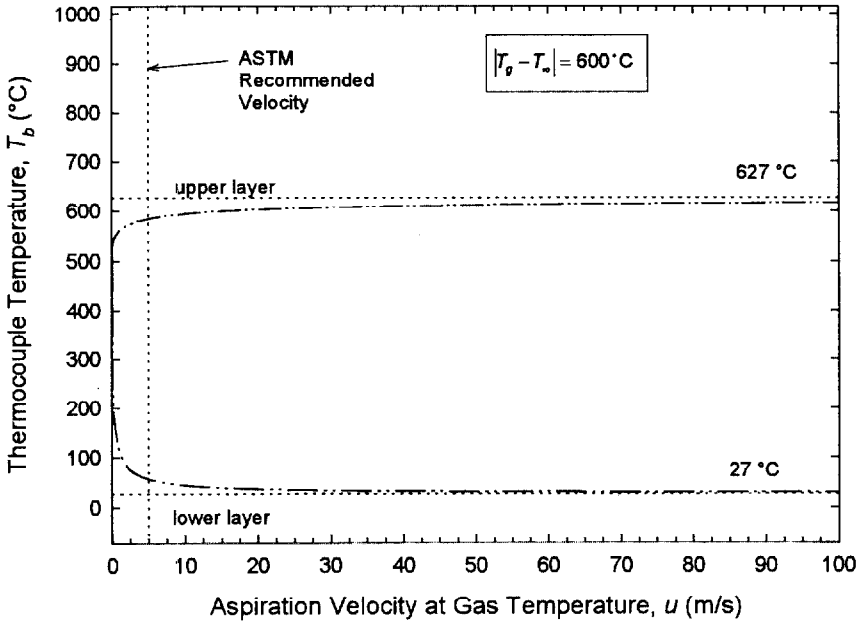

Fig. 8 Predicted single-shielded thermocouple response to variation in aspiration velocity for conditions with differences between T_g and T_∞ of 600 °C. The upper layer case corresponds to T_g = 627 °C and T_∞ = 27 °C, and the lower layer case corresponds to T_g = 27 °C and T_∞ = 627 °C. The vertical line denotes the ASTM-recommended 5-m/s aspiration velocity, and horizontal lines mark the important temperatures of 27 °C and 627 °C.

Figure 9 shows predictions for selected upper and lower layer cases when the difference between T_g and T_∞ is 300 °C. Results for an upper layer case with $T_g = 327$ °C and $T_\infty = 27$ °C are shown along with predictions for a lower layer case with $T_g = 27$ °C and $T_\infty = 327$ °C. These cases signify *low* gas and surroundings temperature differences which might occur during a room fire. As aspiration velocity is increased, the upper layer thermocouple temperature increases suddenly

from its no-aspiration value of 290 °C to 306 °C, and then rises immediately toward T_g (327 °C). The lower layer thermocouple temperature drops from its no-aspiration value of 90 °C to 50 °C, and rapidly approaches T_g (27 °C). For the cases depicted in Fig. 9, the thermocouple temperature approximately equals T_g even for small values of aspiration velocity.

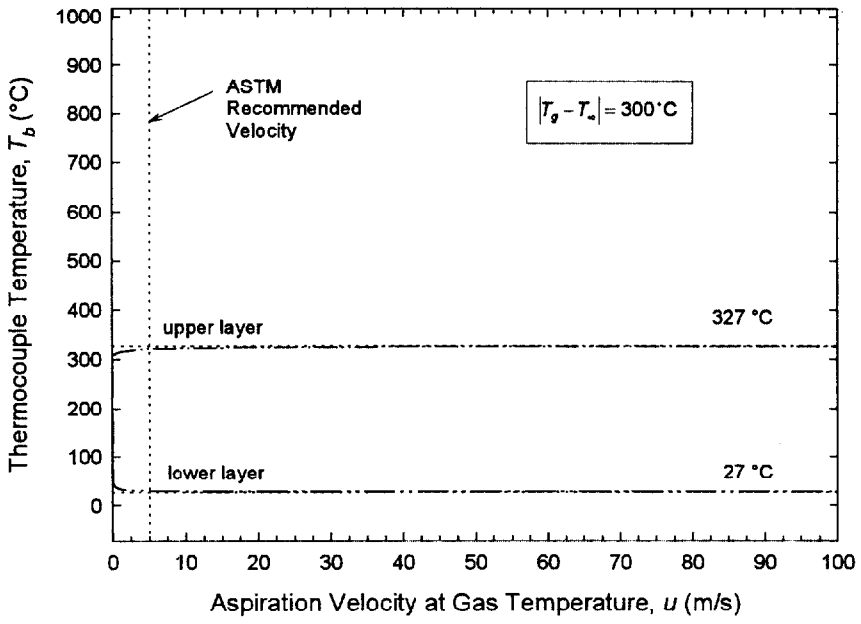

Fig. 9 Predicted single-shielded thermocouple response to variation in aspiration velocity for conditions with differences between T_g and T_∞ of 300 °C. The upper layer case corresponds to T_g = 327 °C and T_∞ = 27 °C, and the lower layer case corresponds to T_g = 27 °C and T_∞ = 327 °C. The vertical line denotes the ASTM-recommended 5-m/s aspiration velocity, and horizontal lines mark the important temperatures of 27 °C and 327 °C.

The results shown in Figs. 7, 8, and 9 demonstrate that the temperature indicated by an aspirated thermocouple approaches the true gas temperature asymptotically as the velocity of the aspirating flow is increased. For low values of $|T_g - T_\infty|$, the thermocouple temperature approaches T_g more rapidly that for higher values of $|T_g - T_\infty|$. As the difference between T_g and T_∞ increases, larger and larger aspiration velocities are necessary to achieve a given accuracy level.

Table I summarizes the thermocouple errors derived from Figs. 7, 8, and 9 for aspiration velocities of 5 m/s, 20 m /s, and 100 m/s. The percents error, defined in terms of absolute temperature as $[\Delta T\,(\mathrm{K})\,/T_g\,(\mathrm{K})]$ x 100 %, are shown in parentheses in the table. Once again, the numerical values of these errors apply only for the specific geometries and parameter choices described in this paper. The numbers are meant to provide order-of-magnitude information, and can be used to qualitatively judge when errors are "small" and when they are "large." For

example, the error of $\Delta T = 213$ °C (or 71 % of absolute gas temperature) for the lower layer case with $T_g = 27$ °C and $T_\infty = 927$ °C is considered "large." The results summarized in the table show that both "small" and "large" errors are possible when the ASTM-recommended 5 m/s aspiration velocity is used during the course of a fire test.

TABLE I. Comparison of predicted thermocouple errors for upper and lower layer cases considered in Figs. 7 through 9. The numbers in parentheses indicate the values of [ΔT (K) /T_g (K)] x 100 %. The value of ΔT in °C is equivalent to the value of ΔT in K, while T_g (K) = T_g (°C) + 273.

Single-Shielded Aspirated Thermocouple Error, ΔT			
	$u = 5$ m/s	$u = 20$ m/s	$u = 100$ m/s
$T_g = 927$ °C $T_\infty = 27$ °C Upper Layer	117 °C (9.8 %)	79 °C (6.6 %)	40 °C (3.3 %)
$T_g = 27$ °C $T_\infty = 927$ °C Lower Layer	213 °C (71 %)	81 °C (27 %)	19 °C (6.3 %)
$T_g = 627$ °C $T_\infty = 27$ °C Upper Layer	42 °C (4.7 %)	24 °C (2.7 %)	10 °C (1.1 %)
$T_g = 27$ °C $T_\infty = 627$ °C Lower Layer	30 °C (10 %)	9 °C (3.0 %)	2 °C (0.67 %)
$T_g = 327$ °C $T_\infty = 27$ °C Upper Layer	6 °C (1.0 %)	3 °C (0.5 %)	1 °C (0.17 %)
$T_g = 27$ °C $T_\infty = 327$ °C Lower Layer	2 °C (0.67 %)	1 °C (0.34 %)	< 1 °C (<0.2 %)

The determination of whether errors of a certain magnitude are acceptable is the responsibility of the individual researcher and will depend on his or her requirements. However, the results summarized in Table I show that the error of an aspirated thermocouple is extremely sensitive to

the value of aspiration velocity. Clearly, the ASTM assertion that 5 m/s is "...sufficiently high to allow accurate temperature measurement based on thermocouple voltage alone, even within flame zones...," can be misleading when the difference between T_g and T_∞ is large, especially in a lower layer, even if the accuracy requirements are only moderate.

The predictions summarized in Table I verify that the practical combustor literature is correct in its assertion that the use of very high aspiration velocities (on the order of 100 m/s) reduces the error of an aspirated thermocouple. However, removing the large quantities of gas necessary to achieve aspiration velocities of 100 m/s is not, in general, practical for fire testing and research. Even if it were possible to produce such high aspiration velocities, Table I demonstrates that a thermocouple could still experience "large" errors for certain conditions (e.g., $\Delta T = 19$ °C for $T_g = 27$ °C and $T_\infty = 927$ °C). Hence, while aspirated thermocouples represent an improvement over bare thermocouples, they should be used with the understanding that they are susceptible to radiation error, especially when operated with low aspiration velocities. This contradicts assertions made previously in the fire literature [3].

4 SUMMARY AND CONCLUSIONS

Heat-transfer models were developed for a bare thermocouple bead, for a single-shielded aspirated thermocouple probe, and for a double-shielded aspirated thermocouple probe. A parametric study was performed. While the absolute values of the errors presented here depend strongly on the configurations studied and the model assumptions, the relative trends between the different fire conditions and instruments allow general conclusions to be drawn.

First, both bare and aspirated thermocouples behave differently in an upper layer of a room fire than in a lower layer. In an upper layer, for a given gas temperature, the thermocouple error is relatively insensitive to surroundings temperature. In a lower layer, much larger errors which increase rapidly with surroundings temperature are possible. The most extreme errors occur in the lower layer when T_g is low and T_∞ is high.

Aspirated thermocouples reduce the magnitude of the errors in the upper and lower layers of a room fire and reduce the likelihood that large errors will occur in the lower layer by shifting the region of large error toward unrealistically high surroundings temperatures. Double-shielded aspirated designs perform better than single-shielded aspirated designs of similar outer diameter. The use of an aspirated thermocouple *reduces* the error, but does not *eliminate* it entirely; the ASTM assertion that 5 m/s is "...sufficiently high to allow accurate temperature measurement based on thermocouple voltage alone, even within flame zones...[24]," can be misleading for certain fire conditions, even if accuracy requirements are only moderate.

The present study provides researchers with the tools necessary to develop steady-state engineering models of bare bead and aspirated thermocouples, tailor them to their own needs, and use them side-by-side with experiments to assess potential measurement errors. The problem then becomes that of selecting values of T_∞, ε, and U which describe the effective radiative and convective environments experienced by the thermocouple throughout the course of a fire. This proves to be a challenging task, because the conditions experienced vary with fire type, with

location in a given fire, and with time at a given location. The models described here are presently being combined with experimental data collected at NIST to gain further insight into the difficult task of performing thermocouple uncertainty analyses in fire environments [4].

Finally, if the uncertainties in thermocouple measurements are to be confidently estimated for fires, future work must address the need to understand the transient radiative and convective environments experienced by each instrument. In the meantime, the type of simplified modeling presented here can provide a great deal of insight for researchers.

ACKNOWLEDGMENTS

The authors acknowledge Emil Braun, Marco Fernandez, Erik Johnsson, Richard Peacock, Paul Reneke, and the staff of the NIST large-scale test facility for performing experiments and for contributing to discussions which provided motivation for this modeling.

REFERENCES

[1] Whitaker, S., Forced Convection Heat Transfer Correlations for Flow in Pipes, Past Flat Plates, Single Cylinders, Single Spheres, and for Flow in Packed Beds and Tube Bundles. *AIChE Journal* **18** (1972) 361-371.

[2] Jones, J.C., On the Use of Metal Sheathed Thermocouples in a Hot Gas Layer Originating from a Room Fire. *Journal of Fire Sciences* **13** (1995) 257-260.

[3] Luo, M., Effects of Radiation on Temperature Measurement in a Fire Environment. *Journal of Fire Sciences* **15** (1997) 443-461.

[4] Pitts, W.M., Braun, E., Peacock, R.D., Mitler, H.E., Johnsson, E.L., Reneke, P.A., and Blevins, L.G., Thermocouple Measurement in a Fire Environment. National Institute of Standards and Technology Internal Report (To Appear), Gaithersburg, Maryland, 1999.

[5] Schack, A., The Theory and Application of the Suction Pyrometer. *The Journal of The Institute of Fuel* **12** (1939) S30-S38.

[6] Mulliken, H.F., Gas-temperature Measurements and the High-Velocity Thermocouple. *Temperature: Its Measurement and Control in Science and Industry*. Reinhold, New York, 1941, p. 775-804.

[7] Mulliken, H.F., and Osborn, W.J., Accuracy Tests of the High-Velocity Thermocouple. *Temperature: Its Measurement and Control in Science and Industry*. Reinhold, New York, 1941, p. 805-829.

[8] Barber, R., Jackson, R., Land, T., and Thurlow, G.G., A Suction Pyrometer for Measuring Gas Exit Temperatures from the Combustion Chambers of Water-tube Boilers. *Journal of the Institute of Fuel* (August 1954) 408-416.

[9] Land, T., and Barber, R.B., The Design of Suction Pyrometers. *Transactions of the Society of Instrument Technology* **6** (1954) 112-130.

[10] Baker, H.D., Ryder, E.A., and Baker, N.H., *Temperature Measurements in Engineering, Volume II*. Wiley, New York, 1961.

[11] Hills, A.W.D., and Paulin, A., The Construction and Calibration of an Inexpensive Microsuction Pyrometer. *Journal of Scientific Instruments (Journal of Physics E)* **2** (1969) 713-717.

[12] Chedaille, J., and Braud, Y., *Industrial Flames, Volume I: Measurements in Flames,* eds. J.M. Beer and M.W. Thring, Crane, Russak, and Company, Incorporated, New York, 1972.

[13] Magidy, P.L., and Lysakov, I.I., Corrections of Local Values of Flame Temperature Measured by Suction Pyrometers. *Heat Transfer—Soviet Research* **7** (1975) 154-160.

[14] Morillon, R., and Perthuis, E., Pyrometres a aspiration: Principes. Realisation d'instruments miniaturises. *Revue Generale de Thermique.* **149** (1974) 399-410.

[15] Khalil, M.B., El-Mahallawy, F.M., and Farag, S.A., Accuracy of Temperature Measurements in Furnaces. *Letters in Heat and Mass Transfer* **3** (1976) 421-432.

[16] Wojtan, M.S., and Jones, K.A.G., Improvements in the design and operation of a suction pyrometer. *Measurement and Control* **14** (1981) 301-305.

[17] Goldman, Y., Temperature Measurement in Combustors by Use of Suction Pyrometry. *Combustion Science and Technology* **55** (1987) 169-175.

[18] Heitor, M.V., and Moreira, A.L.N., Thermocouples and Sample Probes for Combustion Studies. *Progress in Energy and Combustion Science* **19** (1993) 259-278.

[19] Jones, W.P., and Toral, H., Temperature and Composition Measurements in a Research Gas Turbine Combustion Chamber. *Combustion Science. and Technology* **31** (1983) 249-275.

[20] Illerup, J., Dam-Johansen, K., and Glarborg, P., Characterization of a Full-scale, Single-burner Pulverized Coal Boiler: Temperatures, Gas Concentrations and Nitrogen Oxides. *Fuel* **73** (1994) 492-499.

[21] Hughes, P.M.J., Lacelle, R.J., and Parameswaran, T., A Comparison of Suction Pyrometer and CARS Derived Temperatures in an Industrial Scale Flame. *Combustion Science and Technology* **105** (1995) 131-145.

[22] Luckerath, R., Woyde, M., Meier, W., Stricker, W., Schnell, U., Magel, H., Gorres, J., Hartmut, S., and Maier, H., Comparison of Coherent Anti-Stokes Raman-scattering Thermometry with Thermocouple Measurements and Model Predictions in Both Natural-gas and Coal-dust Flames. *Applied Optics* **34** (1995) 3303-3312.

[23] Newman, J S., and Croce, P. A., A Simple Aspirated Thermocouple for Use in Fire. *Journal of Fire and Flammability* **10** (1979) 327-336.

[24] ASTM Standard E 603-98, *1998 Annual Book of ASTM Standards, Volume 04.07.* American Society for Testing and Materials, West Conshohocken, Pennsylvania, 1998, p. 512.

[25] Sparrow, E.M., On the Calculation of Radiant Interchange between Surfaces. *Modern Developments in Heat Transfer.* ed. W.E. Ibele, Academic Press, New York, New York, 1963, p. 181-212.

[26] Modest, M.F., *Radiative Heat Transfer*, McGraw-Hill, Inc., New York, New York, 1993.

[27] Incropera, F.P., and DeWitt, D.P., *Fundamentals of Heat and Mass Transfer, Third Edition.* Wiley, New York, New York, 1990.

[28] Steckler, K.D., Quintiere, J.G., and Rinkinen, W.J., Flow Induced by Fire in a Compartment. National Bureau of Standards Internal Report NBSIR 82-2520, U.S. Department of Commerce, Gaithersburg, Maryland, 1982.

[29] *Omega Temperature Handbook.* Omega Engineering Incorporated, 1996.

[30] In order to adequately describe the choice of model parameters, it is occasionally necessary to identify commercial products by manufacturer's name or label. In no instance does such identification imply endorsement by the National Institute of Standards and Technology, nor does it imply that the particular products or equipment are necessarily the best available for that purpose.

NIST-114 (REV. 6-93) ADMAN 4.09

U.S. DEPARTMENT OF COMMERCE
NATIONAL INSTITUTE OF STANDARDS AND TECHNOLOGY

MANUSCRIPT REVIEW AND APPROVAL

(ERB USE ONLY)

ERB CONTROL NUMBER	DIVISION
G	
PUBLICATIONS REPORT NUMBER	CATEGORY CODE
No. NISTIR 6310	
PUBLICATION DATE	NO. PRINTED PAGES
April 1999	

INSTRUCTIONS: ATTACH ORIGINAL OF THIS FORM TO ONE (1) COPY OF MANUSCRIPT AND SEND TO: WERB SECRETARY, BUILDING 820, ROOM 125

TITLE AND SUBTITLE (CITE IN FULL)
Modeling of Bare and Aspirated Thermocouples in Compartment Fires

CONTRACT OR GRANT NUMBER

TYPE OF REPORT AND/OR PERIOD COVERED
Journal Paper

AUTHORS
L.G. Blevins
W.M. Pitts

PERFORMING ORGANIZATION (CHECK (X) ONE BOX)
[X] NIST/GAITHERSBURG
[ ] NIST/BOULDER
[ ] NIST/JILA

LABORATORY AND DIVISION NAMES (FIRST NIST AUTHOR ONLY)
Building and Fire Research Laboratory, Fire Science Division

SPONSORING ORGANIZATION NAME AND COMPLETE ADDRESS (STREET, CITY, STATE, ZIP)
NIST

PROPOSED FOR NIST PUBLICATION

[ ] JOURNAL OF RESEARCH (NIST JRES)	[ ] MONOGRAPH (NIST MN)	[ ] LETTER CIRCULAR
[ ] J. PHYS. & CHEM. REF. DATA (JPCRD)	[ ] NATL. STD. REF. DATA SERIES (NIST NSRDS)	[ ] BUILDING SCI. SERIES
[ ] HANDBOOK (NIST HB)	[ ] FEDERAL INFO. PROCESS. STDS. (NIST FIPS)	[ ] PRODUCT STANDARDS
[ ] SPECIAL PUBLICATION (NIST SP)	[ ] LIST OF PUBLICATIONS (NIST LP)	[ ] OTHER
[ ] TECHNICAL NOTE (TN)	[X] INTERAGENCY/INTERNAL REPORT (NISTIR)	[ ] —

PROPOSED FOR NON-NIST PUBLICATION (CITE FULLY): [x] —U.S. FOREIGN— [ ]
Fire Safety Journal

PUBLISHING MEDIUM:	[x] PAPER	[ ] DISKETTE	[ ] CD-ROM	[ ] WWW	[ ] OTHER

SUPPLEMENTARY NOTES

ABSTRACT (A 2000-CHARACTER OR LESS FACTUAL SUMMARY OF MOST SIGNIFICANT INFORMATION. IF DOCUMENT INCLUDES A SIGNIFICANT BIBLIOGRAPHY OR LITERATURE SURVEY, CITE IT HERE. SPELL OUT ACRONYMS ON FIRST REFERENCE.) (CONTINUE ON SEPARATE PAGE, IF NECESSARY.)

As part of an effort to characterize the uncertainties associated with temperature measurements in fire environments, models of bare bead, single-shielded aspirated, and double-shielded aspirated thermocouples were developed and used to study the effects of varying the gas and average effective surroundings temperatures on the thermocouple error of each configuration. The models indicate that thermocouples respond differently to changes in effective surroundings temperature in a hot upper layer than in a relatively cooler lower layer of a room fire. In an upper layer, for a given gas temperature, the thermocouple error is relatively insensitive to surroundings temperature. In a lower layer, errors which increase rapidly with surroundings temperature are possible. The most extreme errors occur in a lower layer when the gas temperature is low and the surroundings temperature is high. Aspirated thermocouples reduce the errors in both the upper and lower layers of a room fire, but do not eliminate them entirely. The present study is intended to provide fire researchers with a methodology for developing working models of thermocouples which are tailored to their own configurations.

KEY WORDS (MAXIMUM OF 9; 28 CHARACTERS AND SPACES EACH; SEPARATE WITH SEMICOLONS; ALPHABETIC ORDER; CAPITALIZE ONLY PROPER NAMES)
Instruments; Radiative Heat Transfer; Temperature Measurements; Thermocouples

AVAILABILITY:
[x] UNLIMITED [ ] FOR OFFICIAL DISTRIBUTION - DO NOT RELEASE TO NTIS
[ ] ORDER FROM SUPERINTENDENT OF DOCUMENTS, U.S. GPO, WASHINGTON, DC 20402
[X] ORDER FROM NTIS, SPRINGFIELD, VA 22161

NOTE TO AUTHOR(S): if YOU DO NOT WISH THIS MANUSCRIPT ANNOUNCED BEFORE PUBLICATION, PLEASE CHECK HERE. [ ]